Journal of Electronic Research and Application, 2025, Volume 9, Issue 4
http://ojs.bbwpublisher.com/index.php/JERA
ISSN Online: 2208-3510
ISSN Print: 2208-3502

Optimization Design of Heliostat Field Based on Big Data Technology

Xinyu Wu, Hongjun Zeng, Hewen Wei*

School of Artificial Intelligence, Jianghan University, Wuhan, China

**Author to whom correspondence should be addressed.*

Abstract: In this paper, the optical efficiency and output thermal power of the heliostat mirror field are analyzed and optimized by constructing a geometric model and an optimization algorithm for the optimal design of the heliostat mirror field of a tower-type solar photovoltaic power plant. First, based on the solar position model and the optical efficiency model of the heliostat mirror field, the annual average optical efficiency, the annual average output thermal power, and the annual average output thermal power per unit mirror area of the heliostat mirror field are calculated. Secondly, the EB layout was used to optimize the heliostat field, and the parameters of heliostat size and mounting height were optimized by genetic algorithm and particle swarm algorithm to maximize the annual average output thermal power per unit mirror surface area. The results show that the optimized heliostat mirror field significantly increases the annual average output thermal power per unit mirror area under the condition of achieving the rated power, which provides theoretical basis and technical support for the design and operation of the tower solar thermal power plant.

Keywords: Geometric modeling; Flat projection; Particle swarm algorithm; Genetic algorithm

Online publication: August 7, 2025

1. Introduction

Tower solar thermal power generation, as a clean and renewable energy technology, has received extensive attention in recent years. The heliostat field, as the core component of the tower solar thermal power generation system, its layout and parameter design directly affects the system's power generation efficiency and economy [1]. Traditional heliostat field design methods mainly rely on empirical formulas and simplified models, making it difficult to fully consider the impact of various complex factors on system performance. However, the emergence of big data technology has provided new ideas and methods for the optimization design of heliostat fields [2]. By collecting and analyzing a large amount of actual operation data, the performance of the heliostat field can be more accurately evaluated and optimized, thereby achieving higher power generation efficiency and lower construction costs [3].

1.1. Problem statement

Tower solar thermal power generation utilizes thousands of heliostats arranged on the ground to reflect and concentrate sunlight onto a receiver located at the top of a tower. The receiver converts the concentrated solar radiation into thermal energy, heating the heat transfer fluid inside [4]. Once the fluid reaches a certain temperature, it is transported through pipes to the ground and stored in a high-temperature molten salt tank. During power generation [5], the molten salt is conveyed to the steam generator via a molten salt pump to exchange heat with the feedwater of the steam turbine, generating high-pressure superheated steam to drive the turbine generator set. When the heliostats are in operation [6], the control system adjusts the normal direction of each heliostat in real-time based on the position of the sun, ensuring that the light from the center of the sun is reflected by the center of the heliostat and directed towards the receiver [7]. Building a new power system with new energy as the main body is an important measure for China to achieve the goals of "carbon peak" and "carbon neutrality" [8]. Therefore, we need to maximize the annual average output thermal power per unit mirror area under the condition that the heliostat field reaches the rated power. To achieve this, the following three problems need to be solved:

(1) Given that the absorption tower is located at the center of the circular heliostat field [9], each heliostat has a size of 6 m × 6 m and an installation height of 4 m, and the positions of all heliostat centers are provided, calculate the annual average optical efficiency [10], annual average output thermal power, and annual average output thermal power per unit mirror area of the heliostat field.

(2) Under the condition that the position of the absorption tower remains unchanged, maximize the annual average thermal power output per unit mirror area.

(3) Re-plan the parameters of the heliostat field to maximize the annual average output thermal power per unit mirror area while the heliostat field reaches the rated power.

1.2. Analysis of the problem

The heliostat will actively adjust the azimuth and elevation angles of its mirror surface at any given moment to enable the reflected sunlight to reach the absorption tower [11]. Therefore, the maximum annual average thermal power output per unit mirror surface area is achieved only when the reflected light from the incident light precisely intersects with the lowest point of the absorption tower. At this time, we simulate the energy conversion process of the heliostat field by constructing a geometric model [12]. It can be known that the factors affecting the annual average thermal power output per unit mirror surface area include: atmospheric attenuation, mirror reflection, shadow blocking loss, and overflow loss. By calculating the three types of losses using the flat plate projection method, we obtain the shadow blocking efficiency. This method can improve the calculation speed to a certain extent and obtain the necessary calculation accuracy. We solve the parameters using the obtained data set and actual conditions and formulas [13]. Finally, the parameters obtained represent the annual average optical efficiency, annual average thermal power output, and annual average thermal power output per unit mirror surface area.

Based on the above reasoning, we choose the radiation grid layout method. The heliostats are alternately placed along the isobearing lines at each constant radius, and as the radial distance increases, the arrangement of the heliostat field shows a trend from dense to sparse. Based on the idea of radiation grid arrangement, since adjacent heliostats in the same radial direction will have shadow blocking losses, we can achieve the purpose of avoiding shadow blocking losses by changing the radial spacing position in the near-tower area, adjusting the azimuth spacing layout rules, and considering the geographical location [14]. In this problem, we mainly discuss the case where the absorption tower position remains unchanged, the size of the heliostat is: 2m, 3m, 4m, 5m, 6m,

7m, 8m, and the installation height is the same. In different arrangements of the heliostat, we try to achieve the unobstructed radial spacing as much as possible to maximize the annual average thermal power output per unit mirror surface area.

Finally, within the condition that the mirror surface rotates around the horizontal axis without touching the ground and allowing maintenance and cleaning vehicles to pass smoothly, within a circular area with a radius of 350m, to ensure that the distance between the center of the two towers and the mirror surface is greater than 5m and to maximize the annual average thermal power output per unit mirror surface area (due to the large amount of available data, here we only select a certain amount of data for specific analysis), we select certain data for the mirror surface edge length and installation height, and combine them to obtain data sets - edge length: 3.5m, 4.5m, 5.5m, 6m; installation height: 3m, 4m, 5m, 6m. A total of 6 data sets are obtained for simulation and analysis, and the results are analyzed and compared to obtain the optimal solution.

2. Model establishment

2.1. Model assumptions

Assume that the sunlight is a parallel beam for subsequent calculations; assume that the center of the mirror and the support point of the mirror are coincident; assume that shadows and obstructions only occur within a certain range around the target tracking mirror.

2.2. Model establishment and solution

2.2.1. Data collection and data preprocessing

(1) Data collection

Based on the problem obtained, determine the basic variables such as the solar altitude angle and solar azimuth angle. Use the Python language and the pvlib library in Python to calculate the solar altitude angle and azimuth angle, and store them in the attachment (see Appendix).

(2) Data preprocessing

(a) Establish the horizontal and vertical coordinates of the data and calculate them using Excel formulas.

(b) Based on the solar altitude angle and azimuth angle obtained from data collection, calculate the trigonometric values of the solar altitude angle and azimuth angle, as well as the direct normal irradiance (DNI) using R language.

2.2.2. Establishment of the tracking mirror field coordinate system

Figure 1 shows a "Tracking - mirror coordinate system." In order to describe the positions of the sun and heliostats simultaneously, this paper will use the horizontal coordinate system with the intersection point of the central axis of the heat absorption tower and the heliostat field plane as the origin, as the heliostat field coordinate system. That is, taking the geometric center of the heat absorption tower base as the origin O of the coordinate system, the eastward direction is designated as the positive half-axis of the X-axis, the northward direction is designated as the positive half-axis of the Y-axis, and the zenith direction is designated as the positive half-axis of the Z-axis, to establish a three-dimensional rectangular coordinate system of the mirror field space.

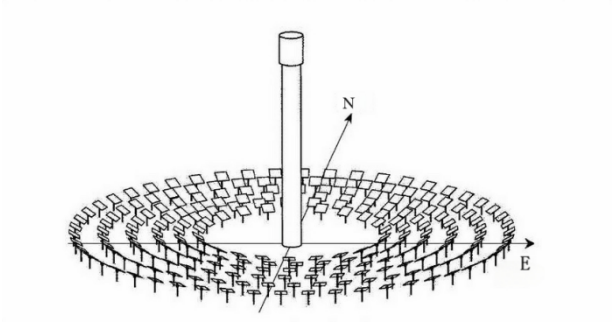

Figure 1. Tracking mirror coordinate system

2.2.3. Solar position model

The solar position model is divided into four dimensions: solar altitude angle, azimuth angle, declination angle, and hour angle. The calculation formulas are as follows:

Solar altitude angle: $\sin\alpha_s = \cos\delta\cos\varphi\cos\omega + \sin\delta\sin\varphi$ (1)

The solar declination (equal to the latitude of the direct solar ray) is denoted by δ, and the geographical latitude of the observation site is represented by (both the solar declination and the geographical latitude are positive for north latitude and negative for south latitude).

Solar azimuth angle: $\cos\ \gamma = \frac{sin\delta - sin\alpha_s sin\varphi}{cos\varphi_s cos\varphi}$ (2)

Solar declination angle：$sin\delta = sin\frac{2\pi D}{365}\sin\left(\frac{2\pi}{360}23.45\right)$ (3)

Here, D represents the number of days starting from the vernal equinox as the zeroth day. For instance, if the vernal equinox falls on March 21st, then April 1st corresponds to D = 11.

Solar hour angle：$\omega = \frac{\pi}{12}(ST - 12)$ (4)

Since the Earth rotates once every day, the size of the solar hour angle corresponding to one hour is 15°. The calculation of the solar hour angle is related to the local longitude and time.

2.2.4. Optical efficiency model of solar tracking mirror field

After the solar light is reflected once by the solar tracking mirror field and propagates to the collector surface, the low-energy-density solar light is gathered into a high-energy-density beam by the solar tracking mirror field, and then converted from solar radiant energy to thermal energy on the collector surface. Among them, the ratio of the energy received by the collector to the total energy of the incident light is called the optical efficiency of the solar tracking mirror field. The optical efficiency of the solar tracking mirror field is affected by factors such as the position of the sun, the arrangement rule of the solar tracking mirrors, atmospheric conditions, the material of the solar tracking mirrors, the geographical location of the power station, and the shape of the collector. It is an important criterion for measuring the concentrating ability of a solar tracking mirror field. Generally, the optical efficiency of the solar tracking mirror field consists of five parts: cosine efficiency η_{cos}, atmospheric attenuation efficiency η_{at}, collector cutoff efficiency η_{trunc}, shadow shading efficiency η_{trunc}, and mirror reflectivity η_{ref}. At any

given moment, the instantaneous optical efficiency of the solar tracking mirrors can be calculated by multiplying the above five parts:

$$\eta = \eta_{sb}\eta_{cos}\eta_{at}\eta_{trunc}\eta_{ref} \quad (5)$$

3. Model optimization comparison

By reviewing the literature, it was found that the mirror field arrangement can be divided into DELSOL layout, EB layout, and No blocking-dense layout. All three layouts limit the mirror field area by resetting the limit factor Arlim for the azimuth spacing, in order to improve land utilization. Moreover, the azimuth angles of the heliostats in the same area are equal, and the azimuth spacing between the heliostats on the same mirror ring is also equal. The performance of the mirror field in both EB and No blocking-dense [15] layout modes is better. Therefore, the EB layout, which has a clearer mathematical model, was selected for optimization research to obtain the coordinate positions of the heliostats.

3.1. EB layout model

Ignoring the influence of terrain on the solar altitude angle and azimuth angle, a calculation formula for unobstructed radial spacing is constructed. This formula is used to build the subsequent model and determine that under the given conditions, the heliostat field reaches the rated power, and the annual average output thermal power per unit mirror surface area reaches the maximum. At this time, the following assumptions are made: the installation height of each heliostat is the same; the size of the heliostat is different; the shadow obstruction between the heliostat and the absorber tower is ignored; the influence of atmospheric refraction and scattering on the solar irradiance is ignored; the heliostat is always facing the sun throughout the day.

Let the longitudinal coordinate of the collector be h, the height of each mirror surface be d, and the reflected light from the mirror surface be M×N. The equation of the light beam can be obtained as: $l_{ij} = f(x_i, y_i, z_i)$,、Let there be U mirrors on the entire plane, that is, there are U×M×N.

The calculation formula for the spacing of the first ring alignment of the tracking mirrors in each area of the mirror field:

$$\Delta A_{\mathrm{Z1,1}} = \Delta A_{Z2,1} = \cdots = \Delta A_{\mathrm{Zi,1}} = A_{\mathrm{sf}} \cdot W_{\mathrm{S}} \quad (12)$$

Except for the first ring, the azimuth spacing of the remaining rings is obtained from the azimuth angles of the tracking mirrors in this area. The calculation formula is：

$$\Delta A_{\mathrm{Z}i,j} = 2R_{i,j} \cdot \sin(\Delta\alpha_{\mathrm{Z},i}/2) \quad (13)$$

The calculation formula for the azimuth angle of the heliostat in the first mirror field area:

$$\Delta\alpha_{\mathrm{Z},i} = 2\arcsin[\Delta A_{\mathrm{Z}i,1}/(2R_{i,1})] \quad (14)$$

The radial spacing between adjacent mirror field areas at their junctions is uniformly set as ΔR = DM. ΔR1,1 represents the radial spacing between the first ring and the second ring of the first area in the mirror field, and the calculation formula is:

$$\Delta R_{1,1} = \sqrt{D_{\mathrm{M}}^2 - (\Delta A_{Z1,1}/2)^2} \quad (15)$$

The working area of the concentrating mirror Arec：

$$A_{\text{rec}} = \pi \cdot (D_{\text{M}}/2)^2 \tag{16}$$

Mirror field area Aland：

$$A_{\text{land}} = \pi \cdot (R_{\max} + D_{\text{M}}/2)^2 \tag{17}$$

The calculation formula for land utilization rate ρ：

$$\rho = A_{\text{rec}} / A_{\text{land}} \tag{18}$$

This results in the average optical efficiency and output power for each month on the 21st.

Table 1. Annual average optical efficiency and output power table

Date	Average optical efficiency	Average cosine efficiency	Average shadow occlusion efficiency	Average truncation efficiency	Average output thermal power per unit area of the mirror surface (kw/m^2)
1/21	0.575842	0.764593	0.974681	0.869715	0.824452
2/21	0.567871	0.761025	0.978465	0.863476	0.835241
3/21	0.586732	0.763086	0.984561	0.859574	0.945623
4/21	0.590124	0.775460	0.971642	0.869654	0.876521
5/21	0.589127	0.775461	0.980012	0.858972	0.945612
6/21	0.585643	0.770102	0.979913	0.869541	0.953214
7/21	0.589916	0.764513	0.974627	0.864755	1.000852
8/21	0.589867	0.765911	0.969842	0.865584	0.965432
9/21	0.585432	0.769895	0.968465	0.867534	0.984575
10/21	0.587462	0.765124	0.974631	0.868473	0.962357
11/21	0.579984	0.764521	0.965579	0.868648	1.000632
12/21	0.576102	0.743578	0.975743	0.864575	0.895641

Table 2. Design parameters list

Absorption tower position coordinates	Diameter of the concentrating mirror (width * height)	Installation height of the concentrating mirror (m)	Total number of heliostat mirrors	Total area of the concentrating mirrors (m^2)
(0,0,84)	8*8	4	1455	93120

Table 2 presents design parameters including the absorption tower's position coordinates, concentrating mirror dimensions, installation height, total number of heliostat mirrors, and total area of concentrating mirrors.

3.2. Genetic algorithm model

It is stipulated that the position of the absorption tower remains unchanged. The side lengths of the fixed solar mirrors are set as: 2m, 3m, 4m, 5m, 6m, 7m, 8m (all in the form of a square); the installation height is set as: 2.5m, 3.5m, 4.5m, 5.5m, 6m; the total number of fixed solar mirrors installed is determined through calculation and

analysis: there are u different sizes of fixed solar mirrors available for selection, among which the size of the nth fixed solar mirror is s_i(i=1,2,3,...,u); there are v different installation heights available for selection, among which the height of the nth installation is.

The equation for constructing is as follows:

Output power of the fixed solar mirror field:

$$E_t = DNI \sum_{i=1}^{u} A_j \eta_i \tag{19}$$

$$A_j = L_i W_i \frac{\sum_{i=1}^{h_i} \sum_{j=1}^{N_j} h_{ij}}{M_i * N_i} \tag{20}$$

Annual average output power:

$$E_{avgf} = \sum_{t=1}^{t=60} E_t \tag{21}$$

Annual average output heat power per unit mirror surface area:

$$E_{avgt} = \frac{E_{favgt}}{\sum si} (t = 1,2,3,\ldots\ldots, \ 60) \tag{22}$$

Among , in order to make as large as possible：

$$\max E = \sum_{t=1}^{t=60} \left| E_{avgt} \right| \tag{23}$$

Since no heliostats can be installed within a 100-meter radius of the absorption tower and the maximum distance of the heliostats does not exceed 350 meters, the geometric relationship is as follows:

$$x_i^2 + y_i^2 \geqslant 100^2, \ \ x_i^2 + y_i^2 \leqslant 350^2 (i = 1, 2, 3 \ldots\ldots u) \tag{24}$$

The width of the mirror surface is equal to the width of the mirror: $H_{si} = W_{sj}$

The length and width of the mirror are between 2 meters and 6 meters: $2 \leqslant d \leqslant 6$

To ensure that the heliostat mirrors do not touch the ground during horizontal rotation：$\frac{1}{2} H_s < d_i$

The distance between the bases of adjacent heliostat mirrors and the distance between the mirror surfaces add up to more than 5 meters:

$$D(u_i, u_j) - \max(H_{si}, W_{sj}) > 5, \ j \neq i$$

By combining the objective functions and using the above data, the genetic algorithm was employed to meticulously integrate and model the formulas and data. After fitting and comparing the analysis results, it was found that the diameter of the heliostat was set as shown in **Table 1**, along with the optical efficiency and output power.

3.3. Result fitting

Figure 2 is a scatter plot showing the coordinate distribution of heliostats, with blue dots arranged in concentric circular patterns on a grid-lined background, having a blank circular area at the center.

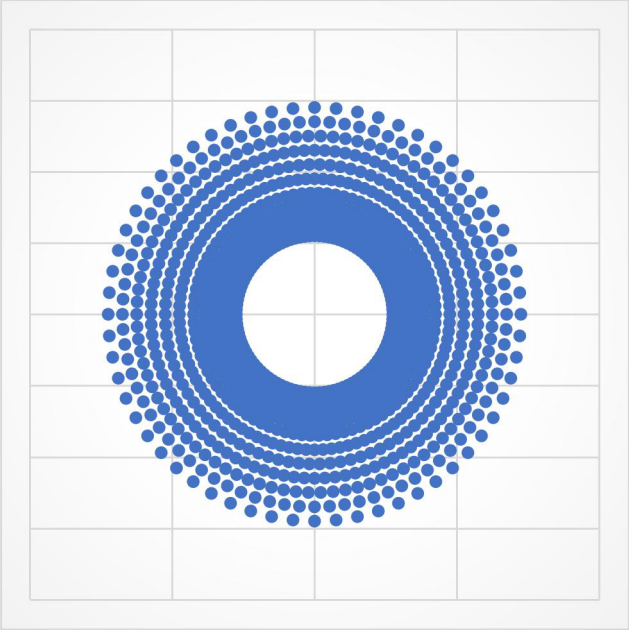

Figure 2. Scatter plot of the coordinate distribution of the heliostats

Table 3 presents the average optical efficiency and output power on the 21st of each month, including metrics like average optical efficiency, average cosine efficiency, average shadow occlusion efficiency, average truncation efficiency, and average output thermal power per unit area of the mirror surface for each monthly date.

Table 3. Average optical efficiency and output power on the 21st of each month

Date	Average optical efficiency	Average cosine efficiency	Average shadow occlusion efficiency	Average truncation efficiency	Average output thermal power per unit area of the mirror surface (kw/m^2)
1/21	0.587665	0.753241	0.985421	0.865147	0.974623
2/21	0.567842	0.762412	0.965423	0.865234	0.975612
3/21	0.598466	0.763225	0.984571	0.854261	0.985614
4/21	0.574787	0.752486	0.968542	0.845621	0.985126
5/21	0581247	0.742859	0.986512	0.849751	0.991256
6/21	0.594821	0.745896	0.965842	0865742	0.972684
7/21	0.588794	0.758612	0.987456	0.874251	0.986254
8/21	0.586743	0.759842	0.976325	0.851698	0.952241
9/21	0.589746	0.756128	0.975126	0.845623	0.975542
10/21	0.589885	0.751802	0.978512	0.849763	0.968854
11/21	0.587155	0.795641	0.976388	0.856941	1.000851
12/21	0.578994	0.789512	0.971261	0.865439	0.996351

Table 4 shows the annual average optical efficiency and output power, listing parameters such as average optical efficiency, average cosine efficiency, average shadow occlusion efficiency, average truncation efficiency, annual average output thermal power, and average output thermal power per unit area of the mirror surface on an

annual basis.

Table 4. Annual average optical efficiency and output power

Average optical efficiency	Average cosine efficiency	Average shadow occlusion efficiency	Average truncation efficiency	Annual average output thermal power (MW)	Average output thermal power per unit area of the mirror surface (kw/m^2)
0.585512	0.760933	0.976783	0.857455	57.695421	0.980417

After calculation, due to the large number of results, here we select five sets of data for presentation:

Table 5 is a design parameters list, providing details like the absorption tower position coordinates, diameter of the concentrating mirror (width * height), installation height of the concentrating mirror, total number of heliostat mirrors, and total area of the concentrating mirrors.

Table 5. Design parameters list

Absorption tower position coordinates	Diameter of the concentrating mirror (width * height)	Installation height of the concentrating mirror (m)	Total number of heliostat mirrors	Total area of the concentrating mirrors (m^2)
(0,0,84)	6*6	5	1455	42382.5

4. Conclusion

This study optimized the heliostat field of tower-type solar thermal power plants by constructing geometric and optical efficiency models, and using EB layout, genetic algorithm, and particle swarm algorithm. Results show that: Optimizing heliostat size (2–8 m) and installation height (2.5–6 m) significantly improved the annual average output thermal power per unit mirror area, with the optimized model achieving 0.9804 kW/m² (annual average) and a maximum of 1.00085 kW/m² in July, alongside higher optical efficiency (0.5855).

The strategy balanced shadow occlusion, truncation losses, land utilization, and operational feasibility (e.g., rotation and vehicle access), providing theoretical and technical support for enhancing plant efficiency and advancing clean energy goals.

Funding

This work was supported in part by the University-Industry Collaborative Education Program under Grant 241006627080140.

Disclosure statement

The authors declare no conflict of interest.

References

[1] 24-Hour Continuous Power Generation! “Clean + Energy Storage + Peak Load Regulation,” Over Ten Thousand Heliostats “Bloom” on the Gobi Desert. CNTV, Channel 13, News Live Room, August 14, 2023, 16:46:23.

[2] Zhang P, et al., 2021, Calculation Method for Optical Efficiency of Solar Tower Concentrated Solar Power Systems. Technology and Market, 28(6): 5–8.

[3] Cai Z, 2015, Sun Shadow Positioning. Mathematical Modeling and Its Applications, 4(4): 25–33.

[4] Du Y, et al., 2020, Analysis of the Impact of Different Focusing Strategies of Tracking Mirrors in Tower-type Solar Thermal Power Plants. Journal of Power Engineering, 40(5): 426–432.

[5] Farges O, Bezian JJ, El Hafi M, 2018, Global Optimization of Solar Power Tower Systems Using a Monte Carlo Algorithm: Application to a Redesign of the PS10 Solar Thermal Power Plant. Renewable Energy, 119: 345–353.

[6] Sun H, Gao B, Liu J, 2021, Research on the Layout of Tracking Mirrors in Tower-type Solar Power Stations. Power Engineering Technology, 42(06): 690–698.

[7] Ding Q, Zeng Z, Chen W, et al., 2021, An Evaluation Method for the Effective Mirror Surface Area of a Concentrating Solar Dish Array. Chinese Journal of Solar Energy, 42(09): 184–189.

[8] Wang X, 2025, Application of Digital Technology in Large-scale Heliostat Construction for Solar Thermal Power Plants. Urban Construction Theory Research (Electronic Edition), (04): 1–3.

[9] Xie Q, Liu G, Liu Y, et al., 2024, Heliostat Field Layout Optimization Method Based on Improved Grey Wolf Algorithm. Acta Energiae Solaris Sinica, 45(11): 394–400.

[10] Li R, Ma S, Jin F, et al., 2024, Optimal Design and Experimental Research on Electromagnetic Variable-Stiffness Dynamic Vibration Absorber for Heliostats. Journal of Vibration and Shock, 43(22): 326–334.

[11] Liu J, Wu J, 2024, Research Progress on Wireless Control Self-Sustaining System for Heliostats in Tower Solar Thermal Power Plants. Solar Energy, (10): 61–69.

[12] Xie H, Zhang J, Li S, et al., 2024, Research on Parameter Model of Heliostat Field Efficiency. Journal of Lanzhou University of Arts and Science (Natural Science Edition), 38(05): 30–36 + 53.

[13] Zhao L, 2024, Research on the Development of Tower Solar Thermal Power Generation Technology. Light & Lighting, (09): 134–136.

[14] Teng D, 2024, Research on Distributed Short-term Irradiance Prediction Method for Heliostat Fields, PhD Dissertation, Xi'an University of Technology.

[15] Zheng C, Lu Y, Hu Y, et al., 2024, Calculation Model for Output Thermal Power of Heliostat Field. Journal of Taizhou University, 46(03): 1–8 + 15.